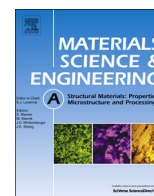




ELSEVIER

Contents lists available at ScienceDirect

Materials Science & Engineering A

journal homepage: www.elsevier.com/locate/msea

Strain rate dependence of the yield stress and strain hardening rate of a single crystal superalloy at intermediate temperature



L.X. Tian, C.L. Ma*

School of Materials Science and Engineering, Beihang University, Beijing, China

ARTICLE INFO

Article history:

Received 11 July 2014

Received in revised form

5 October 2014

Accepted 7 October 2014

Available online 28 October 2014

Keywords:

Strain rate

Strain hardening

Single crystal

Stalking fault

ABSTRACT

The effect of temperature and strain rate on the yield stress and deformation mechanism of the DD6 single crystal is investigated. The results show that the strain rate has very limited effect on the yield stress and strain hardening rate at 873 K, but has strong effect on both properties at 1073 K. The situation at 873 K is similar with the single phase γ' . At 1073 K, the strong strain rate dependence of yield stress is due to the operation of stalking faults. The strain rate dependence of strain hardening rate at 1073 K is attributed to the difference of the dislocation density in the matrix channels.

© 2014 Elsevier B.V. All rights reserved.

1. Introduction

L_{12} compounds which have the Au_3Cu structure usually exhibit anomalous mechanical properties [1]. Since Westbrook showed that the flow properties of Ni_3Al were unusual in 1957 [2], there has been a lot of research aiming at the mechanism of these unusual properties. A great deal of these studies focused on the anomalous temperature dependence of the flow stress and the orientation dependence of the critical resolved shear stress (CRSS) [3,4], however, relatively quite fewer studies were related to the unusual strain rate sensitivity. It is found that some L_{12} compounds, such as Ni_3Al and Ni_3Ga , show a very small positive strain rate dependence when the deformation is carried out by $\{111\}\langle 110 \rangle$ slip system and a strong positive strain rate dependence when the deformation is carried out by $\{001\}\langle 110 \rangle$ slip system [5,6]. The operation of type of slip system depends on the temperature and crystallographic orientation. Most orientations deform by $\{111\}\langle 110 \rangle$ slip system below the temperature of the maximum flow stress (peak temperature) and by $\{001\}\langle 110 \rangle$ beyond the peak temperature except $\langle 001 \rangle$ which deforms only by $\{111\}\langle 110 \rangle$ slip at any temperature [7]. For nickel-base superalloys used at high temperature, they are strengthened by the so-called γ' phase which is based on Ni_3Al . Most of the anomalous properties of the L_{12} compound are inherited. Leverant et al. investigated the strain rate dependence of the CRSS of the single crystal MAR-

M200 superalloy with a $[001]$ tensile axis [8]. They showed that samples deformed below $760^\circ C$, near the temperature of peak flow stress, showed a very small positive strain rate dependence. However, samples deformed at higher temperature exhibited very strong positive strain rate dependence. Leverant et al. suggested that at higher temperature slip was controlled by diffusion processes. The nature of this process was not described, but it was probably related to the diffusion-assisted motion of the dislocations which had cross slipped to the cube planes. This illustration seems unreasonable for the $[001]$ oriented samples, because this orientation is not expected to undergo cube slip as mentioned before. Hirsch et al. did systematic investigation of the strain rate sensitivity of the single phase γ' [9]. They showed that the strain rate sensitivity kept very small and slowly increased with the strain below the peak temperature. Above the peak temperature, Miura et al. showed a strong positive strain rate sensitivity of a $Ni_3(Al,Ti)$ single crystal with $[123]$ orientation at elevated temperatures [10]. This was attributed to the occurrence of $\{001\}\langle 110 \rangle$ slip and the nonplanar core structure of the superdislocation on the cube plane [11]. Nevertheless, this explanation still could not account for the $[001]$ oriented crystals with only octahedral slip at any temperature. Therefore, there should be some difference in the rate-controlling mechanism between the single phase γ' and the double phase γ/γ' superalloys above a temperature threshold. This paper aimed at investigating the different deformation mechanism below and above the temperature threshold ($760^\circ C$ as suggested by Leverant et al.) of a $[001]$ oriented single crystal nickel-base superalloy and its relation to the strain rate dependence of the flow stress and strain hardening rate.

* Corresponding author.

E-mail address: machaoli@buaa.edu.cn (C.L. Ma).

2. Material and experimental procedures

The material investigated in this work is a second generation single crystal nickel-base superalloy DD6 developed by China. The nominal composition of this alloy is listed in Table 1. After being directionally solidified in a Bridgman furnace with the seed technique, the single crystal bars were subjected to a standard heat treatment in order to obtain homogeneous distribution of near cubic γ' phase which was the typical microstructure of nickel-base superalloy in common use. The samples were first homogenised in the single γ phase field at 1290 °C for 1 h plus 1300 °C for 1 h and 1315 °C for 4 h. Subsequently, they were air cooled and aged at 1120 °C for 4 h and 870 °C for 32 h to form the near cubic γ' particles with an average size of around 300 nm.

The samples for compression tests with a gauge length of 6 mm and a cross section of 4 mm•4 mm were machined from the bars by wire-electrode cutting. The initial orientation of the samples was determined by the EBSD technique. The orientation of the compression axis is shown in Fig. 1. The accurate orientation value is [5 18 98] and has an angle of about 10° with the [001] axis.

The compression tests were conducted in air at 873 K and 1073 K with strain rates of 10^{-1} min^{-1} and 10^{-2} min^{-1} . All the tests were interrupted before 2% shear strain for microstructure observation.

For transmission electron microscopy (TEM) observation, deformed specimens were sectioned parallel to the cube plane [010] by wire-electrode cutting. Sliced specimens were mechanically thinned down to about 40 μm with abrasive paper and finally ion thinned to prepare the TEM foils. A JEM-2100F transmission electron microscope was used for observation of the dislocation configuration.

3. Results and discussion

3.1. Compression curves at different temperatures and strain rates

The compression curves of the single crystal DD6 at different temperatures and strain rates are shown in Fig. 2. As mentioned above, all the compression tests were interrupted before reaching 2% shear strain for observation of dislocation configuration.

It can be seen from Fig. 2(a) that the increase of the strain rate has very small effect on the compression curve at 873 K. The 0.2% shear strain flow stress ($\sigma_{0.2}$) increases by less than 10 MPa. In comparison, the single crystal shows large positive strain rate dependence at 1073 K. The $\sigma_{0.2}$ increases by nearly 50 MPa. Another aspect is the remarkable difference in the strain hardening rates. The specimen deformed at 1073 K and 10^{-1} min^{-1} shows a much higher strain hardening rate than all the others.

3.2. Dislocation configuration and the small strain rate sensitivity at 873 K

The small positive strain rate sensitivity is known as an unusual mechanical property of some $L1_2$ crystals such as Ni_3Al and Ni_3Ga [12]. Ezz et al. investigated the strain rate sensitivity of single phase γ' and suggested that the flow stress consisted of two parts $\tau = (2Gb/l_0 + \tau_f) + (\tau_f + aGb/l_0) = \tau_s(T) + \tau_h$

where G is the shear modulus, b is the Burger's vector, l_0 is the length of the Frank-Read source (FR source), τ_f is the long-range

elastic contribution to the stress, l_d is the average distance between obstacles and a is a constant describing the average strength of the obstacles and τ_f' is the strain rate dependent term. Ezz et al. thought that the first part of the stress $\tau_s(T)$ was strain rate-independent and only influenced by the temperature. The small positive strain rate sensitivity was attributed to the second part τ_h which is introduced by some hardening effects. In their theory, the hardening effect is largely controlled by forest dislocations.

The strain rate sensitivity of the $\sigma_{0.2}$ obtained in this work is of the same order of magnitude with the single phase γ' in Ezz's study. Fig. 3 shows some possible dislocation configurations that may be related to local hardening. TEM observation reveals that the dislocation configuration of the specimens deformed at 873 K is almost identical between both strain rates. The images shown in Fig. 3 were obtained from the sample deformed at 873 K and 10^{-2} min^{-1} . The Burger's vectors of these dislocations are very easy to identify when the beam direction is parallel to [010] axis (Fig. 3(d)). Fig. 3(a) shows kinks and bowing segments on dislocation lines. These segments should be bowing out to the cross slip {111} planes rather than cross slip {001} planes, because the specimens are [001] oriented and the resolved shear stress (RSS) on each {001} plane is close to zero. Therefore, these bowing segments may have some effect on the strain hardening, but will not cause strong strain rate sensitivity. Because the core structure of superdislocations in $L1_2$ crystals is planar when slipping on {111} planes and is nonplanar when slipping on {001} plane. The nonplanar core structure of the dislocation on the {001} will introduce strong positive strain rate dependence and the planar core structure on the {111} is almost strain rate independent. Fig. 3(b) shows the intersection of two sets of dislocations. In Fig. 3(c), cross slip between the two slip systems occurred inside a γ' particle as indicated by a white arrow. Pile-up of matrix dislocations is also observed in Fig. 3(c).

It can be deduced from these dislocation configurations in Fig. 3 that (1) dislocation interaction is not very intense at this strain and this temperature; (2) the mobility of the superdislocations is higher than that at 1073 K which will be shown later. If the superdislocation is strongly locked, it will be very straight, but the

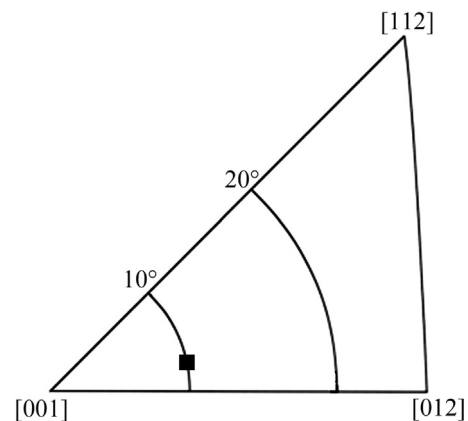


Fig. 1. Initial orientation of the compression samples in the standard stereographic triangle.

Table 1

Nominal composition of the DD6 single crystal superalloy (wt%).

C	Cr	Co	W	Mo	Al	Ti	Fe	Nb	Ta	Re	Hf	B	Ni
< 0.04	4.8	9.5	9.0	2.5	6.2	< 0.1	< 0.3	< 1.2	8.5	2.4	0.15	< 0.02	Bal.

Download English Version:

<https://daneshyari.com/en/article/1574589>

Download Persian Version:

<https://daneshyari.com/article/1574589>

[Daneshyari.com](https://daneshyari.com)